Article:

Dunant, CF, Drewniok, MP, Orr, JJ et al. (1 more author) (2021) Good early stage design decisions can halve embodied CO2 and lower structural frames' cost. Structures, 33. pp. 343-354. ISSN 2352-0124

https://doi.org/10.1016/j.istruc.2021.04.033

Good early stage design decisions can halve embodied CO_2 and lower structural frames' cost

Cyrille F. Dunant[a,*], Michał P. Drewniok[a], John J. Orr[a], Julian M. Allwood[a]

[a] *Department of Engineering, University of Cambridge, Trumpington Street, Cambridge CB2 1PZ, UK*

Abstract

Material efficiency is not currently a common driver of building design. Indeed, in previous studies, we estimated that 12 % of the mass of steel used in structural frames would be saved by more accurate specification of steel members. However, this inefficiency is not the main reason structural frames are light or heavy. We show here for the case of steel structures that it is the layout of the grid and the choice of the decking which have the largest impact on the embodied carbon of frames. Using a database of real designs, associated to a generative design model, we quantify the impact of grid and decking selections. Using our model, we find that real designs are relatively efficient economically, but less so environmentally: the typical building frame could have 40-60 % less embodied carbon, and be approximately 10-20 % cheaper with the right selection. We show how more complex frames have higher embodied carbon than simpler grids. From our findings, we establish a list of design considerations that architects and structural engineers should account for when creating an initial design to lower the embodied carbon: the complexity of the layout, the optimisation of the design and the choice of the decking technology.

Keywords: Efficiency, Design, Steel frames, Optimisation, Design practice, Serviceability

1. Introduction

Civil engineering design sees safety as the overriding concern, with material efficiency often an afterthought, but material efficiency is essential to avoid exceeding a world carbon budget of 580 Gt of co_{2eq} [1]. Construction's carbon footprint is approximately a third of global man-made emissions [2]. A large fraction of this is operational: heating, cooling, and lighting. However, operationally neutral buildings can now be designed, and there is little scope for further operational gains in new builds [3]. Therefore, *embodied* emissions, which can represent up to 60 % of the total in industrial buildings and warehouses, and currently approximately 20 % in office buildings [4, 5], should be targeted for further reduction. The bulk of these emissions is associated with the production of cement, steel reinforcing bars, and

*Corresponding author

steel beams currently driving approximately half of the emissions of industry [6].[1]

The design process is usually constrained by economic considerations, and the most "efficient" solution for the structural designer will frequently be the cheapest option given the requirements. A practical analysis of building design must therefore account for the trade-off between embodied carbon and costs. Crucially, the initial design choices made by the architect or the structural designer can lead to widely different design efficiencies. Fortunately, as materials represent a significant part of the overall budget for the structural frame, heavier structures tend to be more expensive making material efficiency economically attractive in some cases. Understanding the key decisions driving embodied carbon is necessary to provide guidance for lighter building design.

The vertical loads imposed on buildings are applied on its deckings, transmitted to beams and columns, and eventually to the ground through the foundations. Together, with other load transmission elements such as shear walls, these elements are the frame of the building. In structural frames, deckings, columns and foundations represent the bulk of the materials used. The frame's efficiency can be measured in two ways. *The first one* is the easiest to define: each structural element, beam, column, floor plate has a utilisation ratio (UR) which is its limiting (highest) ratio of actual load or limiting frequency or deflection to the one it could bear according to the safety and serviceability criteria defined by the building code. Using this ratio, previous work demonstrated that approximately 15-30 % of the steel in the frame is not required by the construction code in a typical steel-framed building [8, 9]. *The second efficiency measure* compares the overall design with all possible realisations of a given building. It is in principle possible to know these because structural design is highly regulated, with norms effectively describing all the steps required to decide the amount of reinforcing steel and its location, the size of the steel sections, columns and beams used to support the weight of the structure, stability systems, and the design of the foundation.

To establish the *design space* which is the set of all possible realisations of a building, all combinations of the choice of decking technology, material, detailing and layout which satisfy the specifications laid out by the client, structural designer or architect must be considered. These specifications are: the construction bounding box, the number of storeys prescribed, and some architectural features (spans, useful space, permissible depth of floors, loads, usability limit states). Although an infinite number of buildings can be designed which match these requirements, they all lie in a (semi-) bounded space in terms of cost and carbon[2]. Finding the 'best' building performance on the boundaries of this space and comparing it with the actual design is an equivalent of the UR for the whole building.

The problem of generating the design space — all possible combinations of cost and carbon footprint — of buildings

[1]Timber construction is growing and has been touted as more environmentally friendly; however, its associated emissions are not in general significantly lower than that of steel or concrete [7].

[2]It is in principle always possible to design a worse building by adding more unused mass to it.

has not, to our knowledge, been solved. Rather, partial solutions have been proposed. For example a recent paper by [10] proposes a method for the early evaluation of the costs of a frame using fairly detailed knowledge about the layout, which is the hardest element to parametrise. In this work, we use a new model for the assessment of the economic cost and environmental footprint of steel-framed buildings by computing their design space. This framework is built on a computational model of floor plate design. We validate this framework by comparing it to 19 real designs.

We do not do "grid optimisation" in the sense of finding the optimal column locations under a set of constraints. Rather, we compare real designs with models where either the layout is kept the same but the decking and beams are chosen "optimally", or the layout is a simple regular grid using the same decking choice, or both. That way, we can assess the cost in terms of carbon of having an irregular grid layout as well as the consequences of choosing a suboptimal decking.

2. Materials and methods

We use the model described below to explore a number of scenarios (2.4) covering a range of design constraints which the architects or engineers may relax or strengthen and the decision processes which may have led to them. The model aims to find the optimal decking solutions given the geometric constraints and the limit states prescribed so they can be compared to the retained solutions of the case studies (from 2.5). The generated decking geometries used for the selection of decking solutions are generated using the algorithm described in Section 2.1. For each generated plate, the optimal decking (in terms of either cost or embodied carbon) is chosen as detailed in Section 2.2. Cost and carbon models used to evaluate decking designs are described in Section 2.3. A visual representation of a number of technical terms used is found on Figure 1.

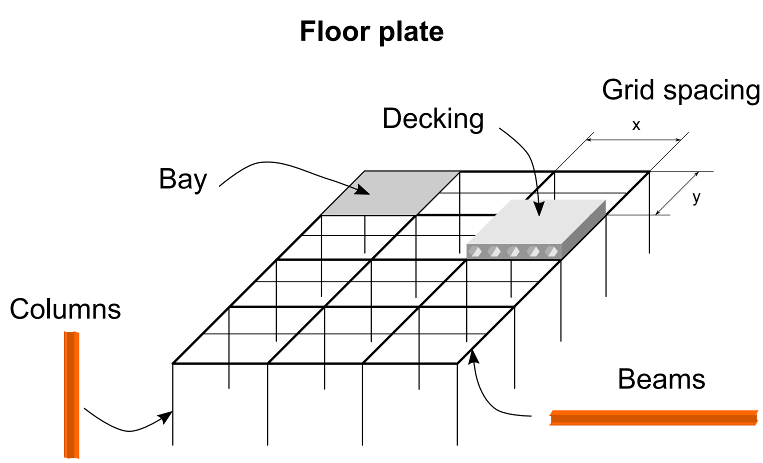

Figure 1: Visual representation of the key concepts and words used to describe a floor plate. Bays are spaces separated by (commonly) four columns, 'decking' refers to the type of floor. Beams and columns are steel I-sections.

2.1. Floor plate generation

The model we use in this paper does not represent floor plates as definite geometries. Rather, bays of the appropriate dimensions are independently generated and designed. Every bay is assumed to be neighboured by a bay which has the average area of all bays in the plate.Some bays are designated “side” or “corner” (which determines the number and location of their neighbours) such that the model floor has the same effective perimeter and area as the design it emulates. Each generated floor thus plate has the same number of bays as the original, with bay dimensions, but with varying layout. The effect of varying the layout is typically small in the case of the steel frame designs studied in this paper. Figure 2 illustrates how a floor plate is decomposed into bays.

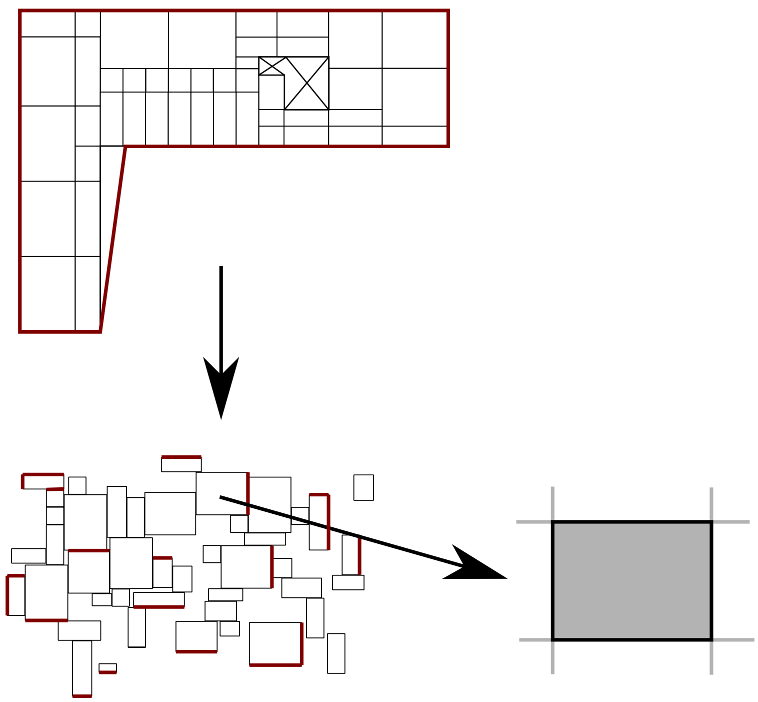

Figure 2: The floor plate is decomposed into its constituent bays. Every bay is then randomly attributed 1, 2, or 4 neighbours, each assumed to have an average size, and design individually.

This approach was validated in a previous work [11] and preserves the overall carbon and cost of the considered floor plates. For each case study (Table 3), at least 500 000 qualitatively equivalent floor plates are generated using our model to estimate the bounds of the design space. This can take for a given set of constraints 12 hours on a desktop computer. Each bay is designed independently for the purpose of beam selection, with the largest span in the floor plate used to determine a single decking type for all the bays.

The algorithm for the generation is as follows, starting with the dimensions of all the bays forming the floor as an input, as read from the plans:

1. Build a queue of all the bays forming the floor. Randomise this queue.
2. Set $\mathcal{A}$ the area of the floor, and $\mathcal{P}$ the perimeter of the floor
3. Pop the first bay from the queue.
4. Select two of its adjacent sides and subtract from $\mathcal{P}$
5. Subtract its area from $\mathcal{A}$
6. *Repeat for all corners*
7. Pop the first bay from the queue.
8. Select one of its sides randomly and subtract from $\mathcal{P}$
9. Subtract its area from $\mathcal{A}$
10. *Repeat until $\mathcal{P}$ reaches 0*
11. Pop the first bay from the queue.
12. Subtract its area from $\mathcal{A}$
13. *Repeat until $\mathcal{A}$ reaches 0*

Most of the variability will come from the location of the bays on the sides and corners of the buildings, as this determines their loading. In general, when generating floor-plates in this way, the exact perimeter of the building being modelled may not be reached. This introduces a small amount of variability in the results, in general in the order of ±£5/m^2 and ±5 kg/m^2 co_2 after cost and carbon have been computed. In all cases if the generated bays have not all been placed, the generated floor plate is discarded and the procedure restarted.

The model does not use information about the neighbourhood of each bays. This avoids the very computationally expensive generation of all possible topological variants of the floor plates. This approach yields a solution where the bill of materials has the same carbon and cost as the real layout as the mass of steel and concrete as well as the number of elements and their average dimensions are conserved. If the original plate was a regular, rectangular grid, the procedure yields the exact result corresponding to the plate, otherwise, we find the result to be within 5 %.

2.2. Structural model

The structural model takes as an input all prescribed limit states as well as the bays generated as above. Loads are shared between bays assuming all bays are bordered by the *average* bay in the structure, accounting for their core, side or corner position.

The design follows the Eurocode 3 and 4 steel design, as described in [12, 13, 14]. The analytical methods therein are used in all cases, although the Eurocode allows for finite element-based design. The Eurocode is sufficiently defined that given a finite set of decking choices, it is possible to find a single less carbon intensive or cheaper option

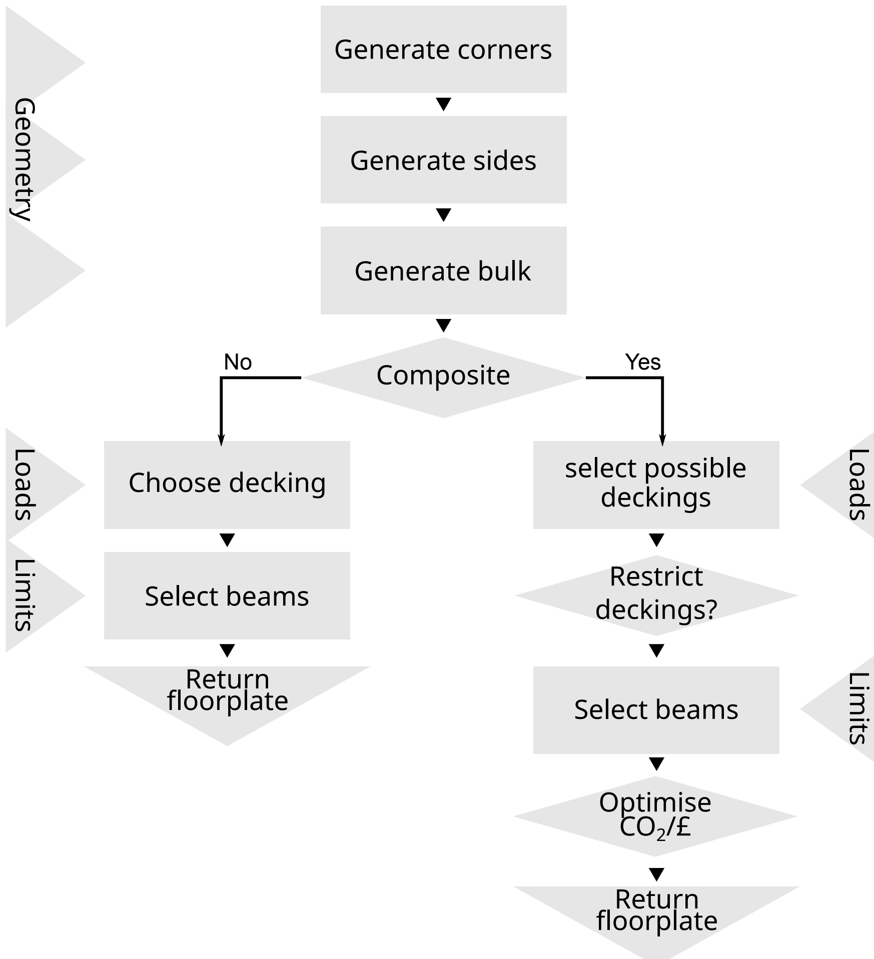

Figure 3: Flowchart describing the generation of floor plates. Composite design needs to distinguish between cheapest and least co_2 intensive options.

given the inputs we have defined. Our model tests all the decking options in its database (Table A.7 in the appendix). Manufacturer's tables are used to determine the possible deckings according to the spans in the floor plate[3]. These give the appropriate steel gauges of profiles and concrete depths according to the load and the mode of construction. It was not possible to determine whether construction was propped or un-propped, un-propped construction was assumed in all composite cases, as it is both more conservative and more common. The fire rating was always assumed to be 60 minutes. Less conservatively, but reflecting common construction practice, the composite deckings assume continuous spans.

Once the decking has been determined, the loads on the beams are known. Beams are selected from the list of

[3]The manufacturers will generally have determined the tables after an experimental programme, and these values almost certainly include a factor of safety. However, it is impossible to determine how large it is, and whether there is much unnecessary embodied carbon in the designs because of this factor.

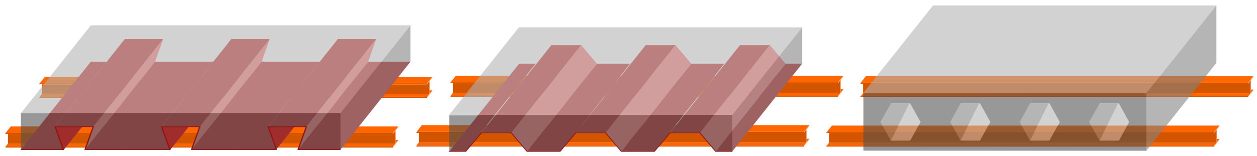

Figure 4: Decking types. From left to right: re-entrant, trapezoidal and precast deckings. 'Primary' beams in composite design then support the secondaries, whereas in precast design 'ties' link the columns.

universal sections found in the appendix for designs using them. This list of universal sections reflects the sections found in the case studies, with $203 \times 102 \times 23$ the smallest beam which fabricators will consider for erection. Such a beam also requires the addition of a bearing plate as it is too narrow for the tolerance of deckings at joints. If the case study used fabricated sections, the model determines the dimensions of the lightest possible welded plate section using the method proposed by [15] to compute the Saint-Venant constant. The beams are selected to be the lightest which will satisfy the limits prescribed for each project, calculated according to [12] for precast, and [14] for composite design.

Finally, the columns required to bear the load of the building are designed and a simple model for the foundations estimates the amount of concrete therein. The costs and embodied carbon in the decking, foundations and columns (designed using the appropriate number of floors) are computed as per 2.3.

2.3. Cost and carbon models

For each floor plate, using the material listing and the decking used, the price and embodied carbon were estimated using the models described below. These models use carbon and cost coefficients from a number of sources as well as the cost structure established by [16]. The coefficients used and calculation methods are given in Table 1. These reflect current values, and will likely change with time. In particular, the price of steel products per tonne has varied over the last ten years from approximately £350 to above £600 [17]. The same coefficients are used in the model and for the evaluation of real designs. To account for the variability of the prices — and uncertainty when evaluating the carbon — the prices and embodied carbon coefficients are varied in each simulation within their uncertainty ranges. When repeating the simulations a large number of times, the results then account for the variations of the input factors.

Because the loads are calculated assuming an average neighbouring bay, the mass of the sections is going to be correct on average. Combined with correct number of sections, this makes the carbon and cost calculations viable.

The cost function for the floor plates is as follows, using the coefficients from Table 1, m_{beam} the mass of the beams, s_{beam} their surface, l_{beam} their length, n_{beams} the number of beams, m_{concrete} the mass of concrete, v_{concrete} the volume of concrete, m_{rebar} the mass of reinforcing steel, m_{decking} the decking steel mass, p_{long} long steel price, p_{plate} the price of

Table 1: Table of cost and carbon intensity coefficients used to model the floor plates. Values for carbon were taken from [18, 19, 20, 21, 22, 23], and for cost, [24, 25, 26, 16]

Description	Cost	Carbon
Concrete	131 £/m^3	137 $\text{kgco}_{2\text{eq}}$/t
Production, construction and transport, depth not exceeding 300 mm. 4.5 % extra volume is assumed to be used on site.		
Rebars	1000 £/t	1380 $\text{kgco}_{2\text{eq}}$/t
Production, construction and transport, average price across rebar sizes		
Composite floor	65–76 £/m^2	As RC+2500 $\text{kgco}_{2\text{eq}}$/t steel
Specific rate depending on type. The steel mass used to calculate the $\text{co}_{2\text{eq}}$ is that of profile and the studs. The RC volume is given by the composite design.		
Rolled steel section	500 £/t	2000 $\text{kgco}_{2\text{eq}}$/t
The price covers only the basic price of the rolled steel, not the fabrication, unlike the carbon		
Fabricated steel section	540 £/t + 290 £/m	2500 $\text{kgco}_{2\text{eq}}$/t
The mass considered should be 4 % larger than the mass of the section, due to cut losses.		
Fabrication (plates and holes)	11% section mass + £240 + 2.6 £/m^2	11% section mass
This includes the end plates, shot-blasting, carcassing, transport and erection. The cost and carbon coefficient depending on mass are those of steel sections.		
Precast slab	54–72 £/m^2	225 $\text{kgco}_{2\text{eq}}$/t + rebar
Specific rate depends on depth, as per [26], 1.75% reinforcement assumed.		

steel plates:

$$\text{beam cost} = m_{\text{beam}} \times 0.11 \times p_{\text{plate}} + 2.6 \times s_{\text{beam}} + \begin{cases} 240 & \text{universal section} \\ 1.04 \times m_{\text{beam}} \times p_{\text{long}} & \text{fabricated plate girder} \end{cases} \tag{1}$$

$$\text{decking cost} = 1.045 \times v_{\text{concrete}} \times 131 + \text{decking rate} \times \text{floor plate area} \tag{2}$$

$$\text{foundation cost} = 1.045 \times v_{\text{concrete}} \times 131 + m_{\text{rebar}} \times 1380 \tag{3}$$

$$\text{total cost} = \text{beam cost} \times n_{\text{beams}} + \text{decking cost} + \text{foundation cost} \tag{4}$$

The carbon function for the floor plates is as follows, using the same coefficients as in Table 1:

$$\text{beam carbon} = 0.11 \times m_{\text{beam}} \times 2300 + 1.04 \begin{cases} m_{\text{beam}} \times 2000 & \text{universal section} \\ m_{\text{beam}} \times 2520 & \text{fabricated plate girder} \end{cases} \tag{5}$$

$$\text{decking carbon} = 1.05 \times m_{\text{concrete}} \times 137 + m_{\text{decking}} \times 2500 + m_{\text{rebar}} \times 1380 \tag{6}$$

$$\text{foundation carbon} = 1.05 \times m_{\text{concrete}} \times 137 + m_{\text{rebar}} \times 1380 \tag{7}$$

$$\text{total carbon} = \text{beam carbon} \times n_{\text{beams}} + \text{decking carbon} + \text{foundation carbon} \tag{8}$$

2.4. Scenarios

We considered a number of scenarios describing various design strategies. All scenarios were tested assuming both target URs of 0.8, as per [9] and 1.0. Deckings types all exist in a number of variants, with variable depth of concrete and thickness of steel. Optimising decks means choosing the thinnest steel and concrete layer which will satisfy the design constraints. Decks are classified in categories: re-entrant, trapezoidal, and precast. Choosing amongst these correspond to other constraints such as the overall depth of the structural layer or aesthetics. Vendors propose similar deckings which each perform best in particular circumstances, but are otherwise quite similar. The flowchart of decisions leading to the choice of a particular decking is illustrated on Figure 5. In many practical cases, the designer cannot specify the vendor of the decking, and that decision will be made by the main contractor or the fabricator.

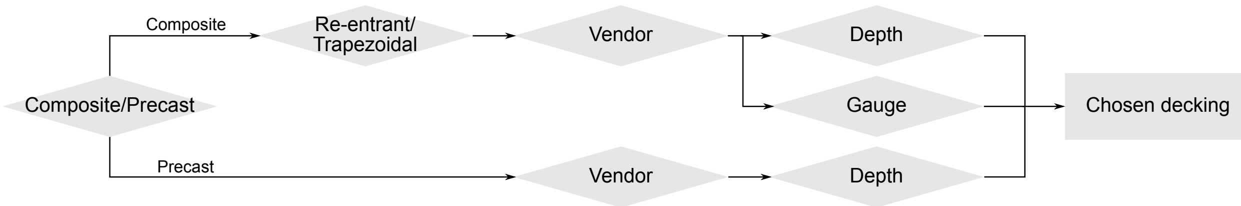

Figure 5: Decision flowchart leading to the choice of a deck. The choice of the gauge and depth depends on structural constraints as well as acoustic and architectural considerations, which are not accounted for in the model. The other choices may depend on geometric limits or commercial considerations.

The scenarios considered are:

Optimised deck (D, DO) this uses the same decking type, from the same vendor as the corresponding case studies, but uses the optimal steel gauge and concrete depth. This scenario matches the spans and bay size distribution of the real buildings.

Optimise and choose best deck within category (DC, DCO) In this scenario, the choice of decking is constrained only to the same general decking type (composite re-entrant or trapezoidal or precast) that was chosen in the real designs. This scenario matches the spans and bay size distribution of the real buildings.

Optimise deck chosen within all options (DA, DAO) In this scenario, the choice of decking is unconstrained. Both precast and any composite option can be chosen, from any vendor.

Grids (G, GO) this scenario uses a single bay type throughout with a target UR of 0.8, representing the effect of choosing simpler layout over more complicated ones. The resulting buildings have the same area and perimeter as the corresponding case studies.

Don't design for frequency SLS (F, FO) is identical to the first 'Optimised deck' scenario which closely matches the case studies, but the frequency check for the beams is omitted. The role of the frequency check was investigated because it frequently dominates design, despite not being a code requirement, and its value being poorly correlated to real-world performance. Although not a code requirement, the structural engineers use the guidance on frequency as a limit in much the same way they do ULS limits (Figure 9).

Together, these scenarios explore the effect of the decking choice, the role of the frequency checks, that of the beam optimisation and the effect of layout complexity. The coupled roles of factors could be investigated by combining the results of scenarios following Table 2.

Table 2: Summary table of the cross comparison of the various effects considered using the results from the different scenario, whether by comparing scenarios (⇆), or looking at the scenarios themselves↺.

	Complexity	Optimisation	Decking choice	Freq. check
Complexity	G⇆D	G⇆GO	G↺	—
Optimisation	G⇆GO	D⇆DO	D⇆DO	F⇆FO
Decking choice	G⇆GO D⇆DO	D⇆DO	D⇆DC⇆DA DO⇆DCO⇆DAO	F↺
Freq. check	—	F⇆FO	F⇆D FO⇆DO	F↺

2.5. *Case studies*

We extracted from a database of floor plate designs the designs which reached construction (from [9]). The 19 selected designs are listed in Table 3. These provide a good coverage of commercial and public sector buildings, as well as decking designs.

Table 3: Overview of the case studies. Sectors are Commercial (Com), Education (Edu). All case studies are from the UK.

#		Year	Stage	Storeys	Height	Decking type
1	Com	2005	As Built	13	50.0	Trapezoidal
3	Com	2006	Construction	5	17.5	Pre-cast
4	Com	2013	Construction	3	12.0	Re-entrant
5	Com	2010	Construction	6	21.8	Re-entrant
6	Com	2008	Construction	3	11.0	Re-entrant
8	Com	2006	Construction	5	23.3	Trapezoidal
9	Com	2001	Construction	3	11.4	Trapezoidal
10	Edu	2016	As Built	3	11.8	Pre-cast
13	Edu	2012	Construction	3	11.6	Trapezoidal
14	Edu	2016	Construction	2	7.7	Re-entrant
15	Edu	2006	Construction	3	9.3	Pre-cast
16	Edu	2013	Construction	2	7.6	Trapezoidal
17	Edu	2005	Construction	3	11.2	Re-entrant
19	Edu	2016	Construction	2	6.3	Trapezoidal
20	Edu	2014	Construction	3	12.6	Trapezoidal
21	Edu	2013	Construction	3	11.6	Trapezoidal
22	Edu	2014	Construction	2	8.7	Pre-cast
24	Com	2014	Construction	1	5.9	Trapezoidal
27	Com	2016	Construction	2	5.7	Pre-cast

The prescribed loads are known for each building design, and have been used for the analysis. The cladding loads, however, are not known. They have been assumed to be 20 kN/m for every building[4]. The ultimate and serviceability limit states (ULS and SLS) are known from the designs, as well as the steel grade of the beams, and are used in the model

[4]This value was given as typical by structural engineers during interviews.

to compute the solutions.

3. Results

The analysis we conducted using our model aimed at determining the potential for lower embodied $\text{co}_{2\text{eq}}$ in the case studies by altering design choices. We compared the embodied $\text{co}_{2\text{eq}}$ and costs of the actual designs and generated ones having either the same distribution of bay sizes or regular grids, varying target utilisation ratios and SLS limits. The model designs are always optimised twice, for both cost and embodied carbon. As the results optimising for cost also have in general lower carbon than the case studies, we only report those below.

3.1. Simulations results

The design spaces generated by the model and their relation to real designs in the different scenarios are illustrated in Figure 6. This figure illustrates how relaxing the different design constraints expands the options available to the structural designer, from using the same decking, to similar deckings, to any decking to freely choosing the grid.

Table 4 shows the decking choice from the model versus the design choice when the decking type is kept the same in the model and designs. This indicates that heavier gauges are commonly chosen, but most importantly that the amount of concrete used is not justified for strictly structural reasons in many cases. This may be because in the designs architectural screeds were specified: these serve no structural purpose, but allow more flexibility in shaping the floors. Other possible reasons for thicker concrete covers include thermal and acoustic insulation, and thermal comfort.

Table 4: Comparison between optimal model solutions and real design solutions when the choice of trapezoidal versus re-entrant decking is imposed. The larger values in either model or design have been highlighted in bold.

			Model		Design	
#	Decking		Gauge	Concrete	Gauge	Concrete
1	Trapezoidal	60	0.90 mm	120 mm	**1.00 mm**	**140 mm**
3	Precast			250 mm		250 mm
4	Re-entrant	51	0.90 mm	100 mm	0.90 mm	**150 mm**
5	Re-entrant	51	0.90 mm	100 mm	**1.20 mm**	**130 mm**
6	Re-entrant	51	0.90 mm	100 mm	**1.20 mm**	**130 mm**
8	Trapezoidal	60	0.90 mm	100 mm	0.90 mm	**130 mm**
9	Trapezoidal	80	0.90 mm	140 mm	**1.00 mm**	**150 mm**
10	Precast			**300 mm**		250 mm
13	Trapezoidal	60	0.90 mm	130 mm	**1.10 mm**	**150 mm**
14	Re-entrant	51	0.90 mm	100 mm	**1.10 mm**	**130 mm**
15	Precast			150 mm		150 mm
16	Trapezoidal	60	0.90 mm	120 mm	**1.00 mm**	**150 mm**
17	Re-entrant	51	0.90 mm	100 mm	**1.20 mm**	**130 mm**
19	Trapezoidal	60	0.90 mm	100 mm	**1.00 mm**	**150 mm**
20	Trapezoidal	60	0.90 mm	120 mm	**1.20 mm**	**130 mm**
21	Trapezoidal	60	0.90 mm	120 mm	**1.00 mm**	**150 mm**
22	Precast			200 mm		200 mm
24	Trapezoidal	80	0.90 mm	140 mm	**1.20 mm**	**150 mm**
27	Precast			200 mm		200 mm

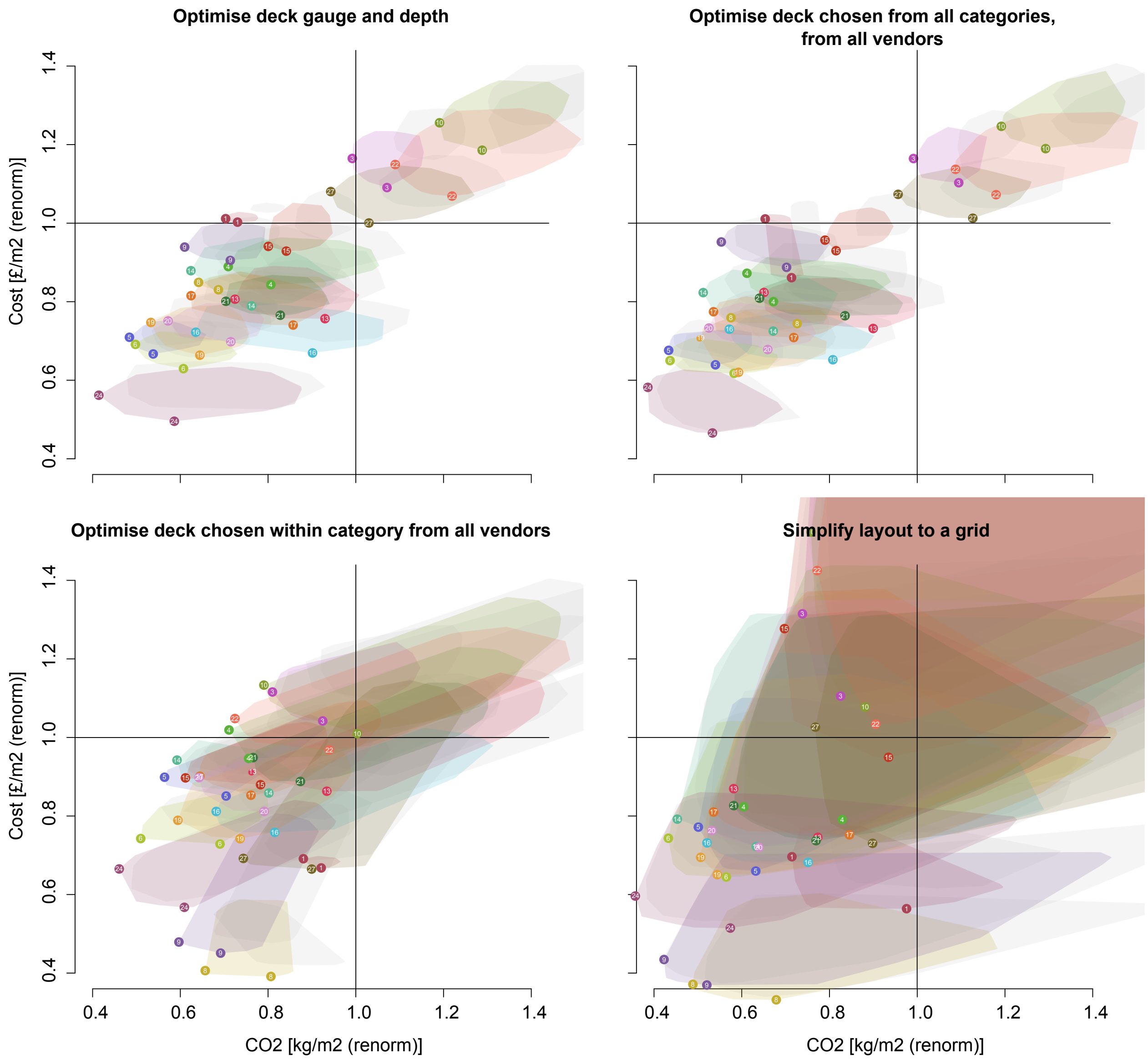

Figure 6: Design spaces generated by drawing the convex hull of all generated solutions plotted in the cost-carbon space (coloured shapes). The optimal cost and the optimal carbon design in each case are marked using filled circles. The grey shadows indicate the location of the design spaces assuming a target UR of 0.8.. Relaxing the design constraints allows for more optimal solutions. The plot correspond to carbon-optimised deckings, with a target UR of 1. In light gray, the corresponding results with a target UR of 0.8. As the constraints on the design are successively relaxed, allowing for more variance from the initial design, the design spaces grow.

Table 5 shows the difference in choice of decking between the optimal choice according to the model and the actual designs. In all cases composite designs are selected by the model over precast, although this proportion possibly reflects the selection of case studies. When they are the same type, the composite designs are almost always lighter in the model, using lighter gauges and shallower concrete layers. The price difference between model and case study is less because the number of beams, driving approximately two thirds of the price, is largely the same. Trapezoidal deckings are always favoured over re-entrant composite design which is disadvantaged due to the code calculation of the shear connection factor.

Table 5: Comparison between optimal model solutions and real design. The larger values in either model or design have been highlighted in bold.

#	Model				Design			
	Decking		Gauge	Concrete	Decking		Gauge	Concrete
1	Precast			300 mm	Trapezoidal	60	1.00 mm	140 mm
3	Trapezoidal	60	1.00 mm	120 mm	Precast			260 mm
4	Trapezoidal	60	0.90 mm	120 mm	Re-entrant	51	0.90 mm	**150 mm**
5	Trapezoidal	60	0.90 mm	120 mm	Re-entrant	51	**1.20 mm**	**130 mm**
6	Trapezoidal	60	0.90 mm	120 mm	Re-entrant	51	**1.20 mm**	**130 mm**
8	Trapezoidal	60	0.90 mm	120 mm	Trapezoidal	60	0.90 mm	**130 mm**
9	Trapezoidal	60	0.90 mm	120 mm	Trapezoidal	80	**1.00 mm**	**150 mm**
10	Trapezoidal	60	0.90 mm	120 mm	Precast			250 mm
13	Trapezoidal	60	1.10 mm	120 mm	Trapezoidal	60	1.10 mm	**150 mm**
14	Trapezoidal	60	0.90 mm	120 mm	Re-entrant	51	**1.10 mm**	**130 mm**
15	Trapezoidal	60	0.90 mm	120 mm	Precast			150 mm
16	Trapezoidal	60	1.00 mm	120 mm	Trapezoidal	60	1.00 mm	**150 mm**
17	Trapezoidal	60	0.90 mm	120 mm	Re-entrant	51	**1.20 mm**	**130 mm**
19	Trapezoidal	60	1.20 mm	120 mm	Trapezoidal	60	**1.00 mm**	**150 mm**
20	Trapezoidal	60	0.90 mm	120 mm	Trapezoidal	60	**1.20 mm**	**130 mm**
21	Trapezoidal	60	0.90 mm	120 mm	Trapezoidal	60	**1.00 mm**	**150 mm**
22	Trapezoidal	60	0.90 mm	120 mm	Precast			200 mm
24	Trapezoidal	60	0.90 mm	120 mm	Trapezoidal	80	**1.20 mm**	**150 mm**
27	Trapezoidal	60	1.10 mm	120 mm	Precast			200 mm

Figures 7 and 8 shows how the modelled floor plates compare to the real designs in the scenarios tested. The 'Optimise deck' scenario assuming a target UR of 0.8, corresponds to the observed design practice [9]. Nearly all designs have the potential to be both cheaper and less carbon intensive. Optimisation is nearly always possible even when the target UR is 1. The most dramatic savings potential comes from simplifying the floor plates to simple grids.

Allowing a wider choice of decking technologies reduces the variability of the optimisation potential (Figure 7). Thus, in some instances the choice of technology not adapted to the floor plate layout. This also shows that it should be possible to legislate embodied carbon limits without prejudice to architectural design as tight carbon limits seem achievable.

Table 6: Impact of each factor. Min and max result from optimising or not the UR to 1 in conjunction with the factor.

Factor	**Relative [%]**				**Absolute [£/m^2, kgCO_2/m^2]**			
	Cost impact		Carbon impact		Cost impact		Carbon impact	
	[mean	min – max]			[mean	min – max]		
Decking optimisation	13	—	22	—	43	29—62	79.5	59—100
UR optimisation	3.8	3.0—4.6	7.0	3.4—8.4	5.1	3.9—6.4	11	4.4—14
Decking choice	3.6	3.4—3.9	7.0	6.6—7.4	6.8	6.3—7.3	12	11—13
Decking tech choice	4.7	4.4—5.0	5.7	5.5—5.9	15	15—16	6.7	6.2—7.2
No frequency limit	4.4	4.2—4.6	8.7	8.1—9.3	7.9	7.5—8.3	15	13—16
Grids	13	12—13	21	19—23	28	28—29	33	28—38

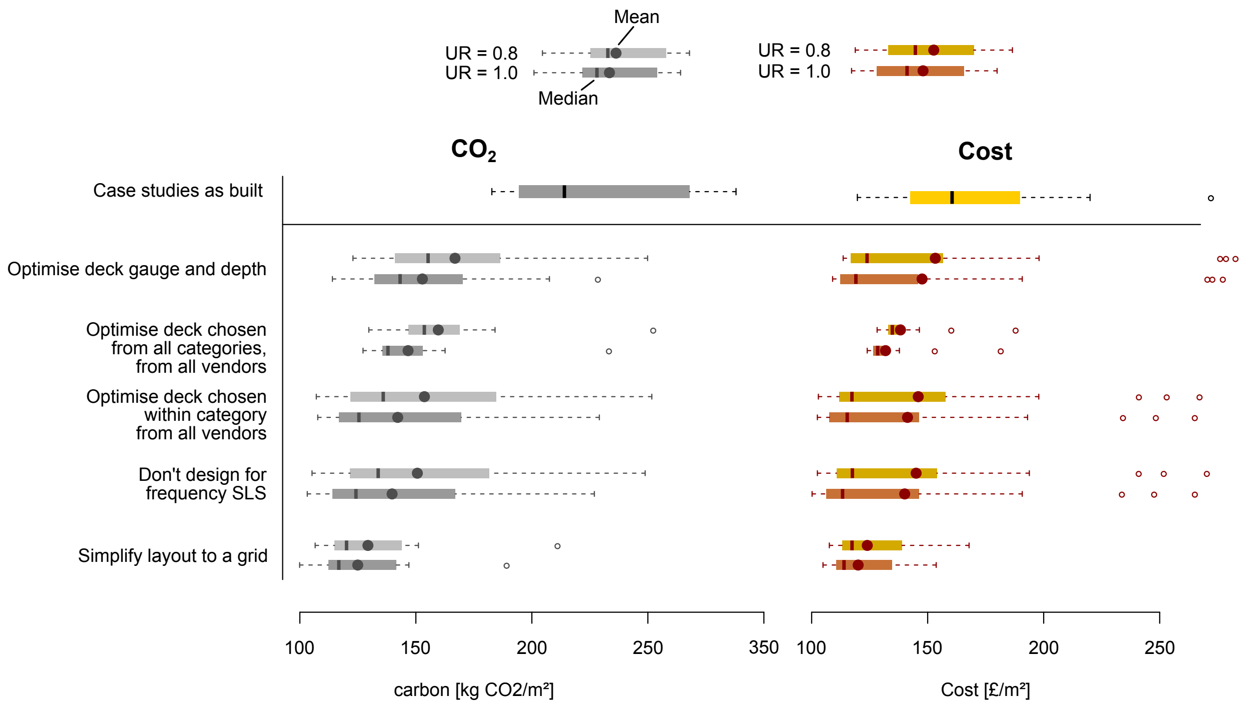

Figure 7: This figure illustrates the distribution of optimisation potential depending on the different scenarios.

Ignoring the frequency SLS brings similar benefits to optimising beams. This may indicate that this commonly dominating design feature is detrimental to the quality of design. Indeed, computing the natural frequency of bare floors is not very useful in practice: the real frequency tends to be determined by the location of partitions, which are not accounted for in decking design. There exist better ways to determine the vibration behaviour of floor, and these may yield different results than what we present here.

The 'Grids' scenario highlights the cost of using more complex architectural forms. Variability in bay sizes can be a source of heavier design as grids are typically 50 % lighter than the more complex designs and 25 % cheaper. This is because the overall design is more likely to be dominated by a few unfavourable bays.

4. Discussion

Figure 9 shows the most common SLS utilisation ratio is around 0.85 for deflection, but 0.75 for frequency. The difference in the distribution of the deflection and frequency UR may indicate that designers, although in both cases more defensive than the code requires, consider their frequency calculations less certain than their deflection calculations. This uncertainty is reflected by practice, where the location of the partitions and the loading of the floor dominate the behaviour of the floor. This suggests a need to understand real SLS behaviour and convert this into guidance that is usable for designers.

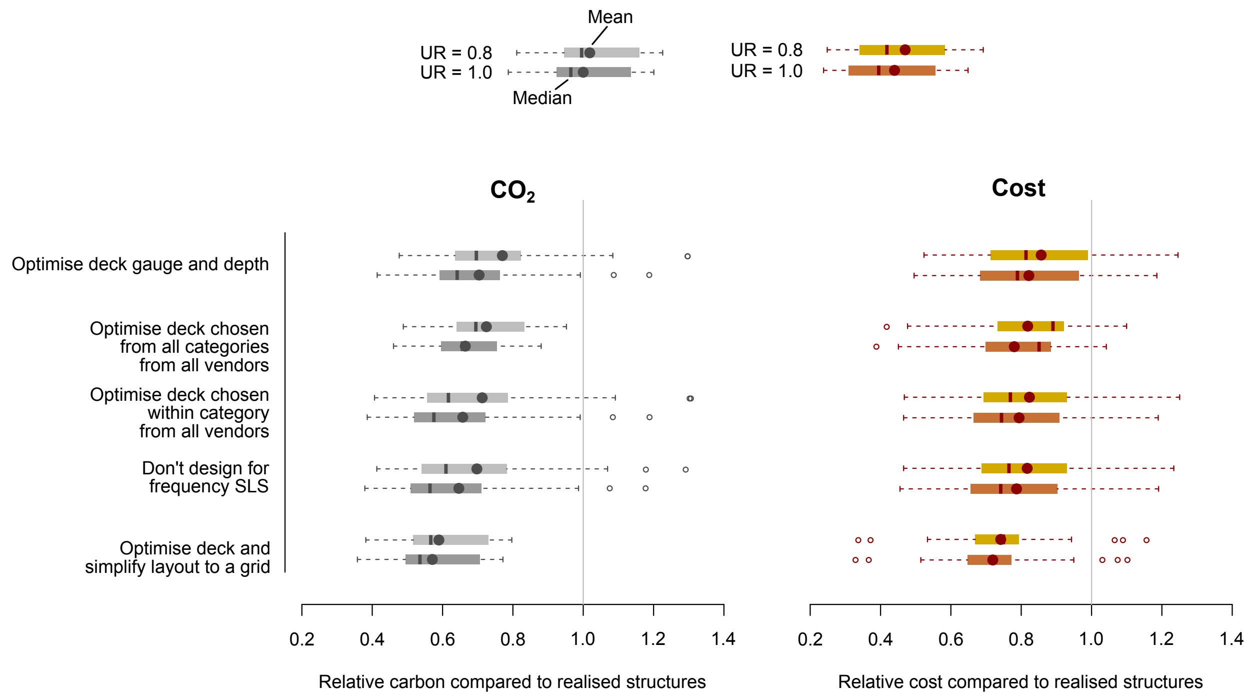

Figure 8: This figure illustrates the distribution of optimisation potential relative to the embodied costs and carbon of the case studies depending on the different scenarios.

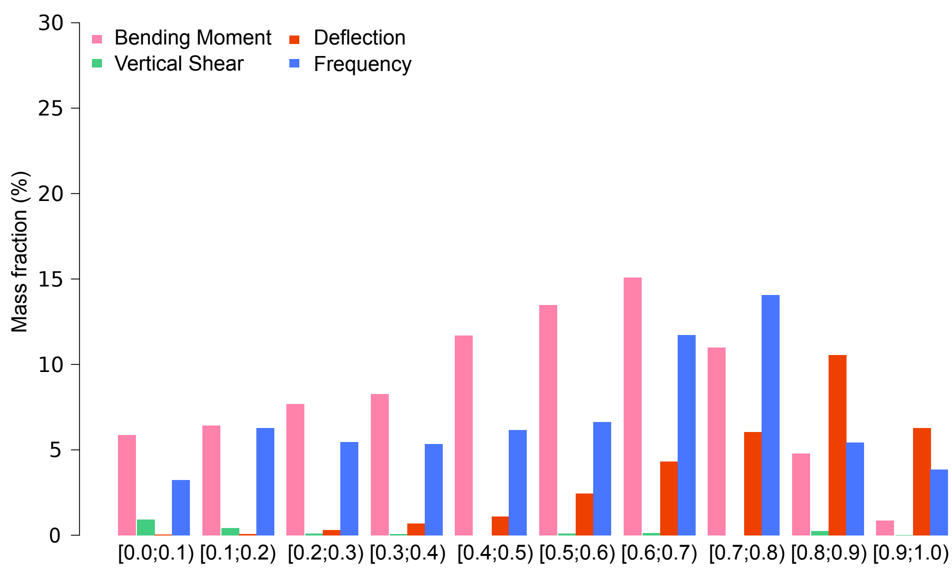

Figure 9: Comparison between the serviceability UR and the ULS limit state. The most common UR, following the findings of [9] is 0.8, reflecting defensive design practice.

As found by [9], the complexity of the floor plate design relates strongly to their embodied carbon. This is obvious when looking at the optimisation potential offered by using regular grids rather than the actual layouts of the building in Figure 7. Grids are not dominated by the 'worst' bay in the grid for the choice of the decking, rather, the decking can be better optimised for the load case and the spans. Further, the reduced complexity translates to reduced costs. In the case of simpler designs, the benefits are lower, indicating that more complex designs benefit more from optimisation. Of course, the shape of buildings is not complex because of the whims of the designers: the constructible surface may have an odd shape, and its use should be maximised. But frequently also, architectural drive towards 'interesting' buildings will introduce quirks in the design which are detrimental to the efficiency. We do not suggest that buildings should be designed as perfectly regular boxes, but we find that a rationalisation effort, with a preference for regular grids generally improves the material utilisation of buildings.

The combined selection of a thicker steel gauge and deeper layer of concrete explain the difference in cost and carbon between the case studies and their simulated counterparts. Although the real designs are perhaps 20 % more expensive than what the model suggests they could be, they are nearly 50 % more co_{2eq} intensive due to a combination of the choice of decking and under-optimisation of beams. In practice the type of decking will have been chosen very early in the process, based on expertise and experience. As seen in Table 5, re-entrant decks are used very commonly, despite being less efficient than trapezoidal ones. The minimum shear connection required for trapezoidal decks is (η the minimum shear connection required, M_{ed} the design moment, and M_{res} the moment capacity of the steel member):

$$\eta = \max\left(0.25 \quad ; \quad 0.3\frac{M_{\text{ed}}}{M_{\text{res}}}\right) \tag{9}$$

Whereas for re-entrant it is:

$$\eta = \max\left(0.28 \quad ; \quad 0.4\frac{M_{\text{ed}}}{M_{\text{res}}}\right) \tag{10}$$

a higher baseline [27]. In general, the requirement for the minimum shear connection is higher for re-entrant decks. This may explain why re-entrant decks are less favoured by the algorithm.

This choice is justified because they are slightly thinner in principle. The concrete depth is larger in the designs than in many of the models, thus this potential benefit is commonly lost in practice. Importantly, when imposing the decking choice in the model to match the case studies, the choice of the decking variant is systematically heavier than required. The choice of the decking also has knock-on effects.

The decking imposes a significant load on the beams — and in the case of composite design may determine which beams can be chosen for the construction stage. This extra load tends to lower the natural frequency, requiring stiffer beams, which are also frequently heavier. In discussions, we found that engineers believe quite strongly that the 60 mm trapezoidal and 51 mm re-entrant decks are the default choices for design, and indeed these are the best selling options [28]. However, the simulations indicate that the 80 mm trapezoidal decks are frequently better choices, suggesting engineers should expand the selection of deckings considered for designs.

There is currently considerable scepticism in the academic community that the building design codes [29, 30] are conducive to lean designs, and this scepticism is reflected in the construction industry. Optimisation techniques using genetic algorithms or gradient descent can take an existing design and produce from it better designs which still satisfy the requirements of the original building (see *e.g.* [31, 32, 33]). Such techniques are somewhat limited in that they only work well for a single technological choice, or are applicable only at the scale of a single structural element, and not the whole building. They are rarely used in practice, largely for prestige projects pushing the boundaries of engineering and not for the bulk of constructions where the potential for greenhouse gas emissions mitigation is the highest (for example, in [34]). Rather, building better buildings in common practice is a matter of engineers making the right technological choices more often, and architects and clients having better understanding of the environmental and economic trade-offs implicit in their choices of layout and function.

5. Conclusions

We used a database of real designs to explore the drivers of material efficiency in steel construction. We found that the aspects which should be considered first by engineers wishing to produce low-embodied-carbon buildings are (Figure 10):

1. choosing and keeping regular grids wherever possible,
2. choosing carefully their decking technology,
3. optimising the beams to UR= 1 once the design is finalised.

The method used to compute the natural frequency in this paper is a simplified one. There are better methods, making use of finite element simulations which are available and could be used. Nonetheless, as a first-order approximation, the method used here is widely employed and the results suggest this is detrimental to the efficiency of designs.

Potential material savings of around 50 % are common [35]. 50 %, is also quite close to the potential saving in cement use in the UK, calculated through completely different means [36]. That this number be driven by the initial choice of technology is encouraging: early choices in the design process can have large positive impacts on the final result and are, in principle, cheap to make.

Acknowledgements

We would like to warmly thank Price & Myers for their invaluable help in this analysis and their expertise.

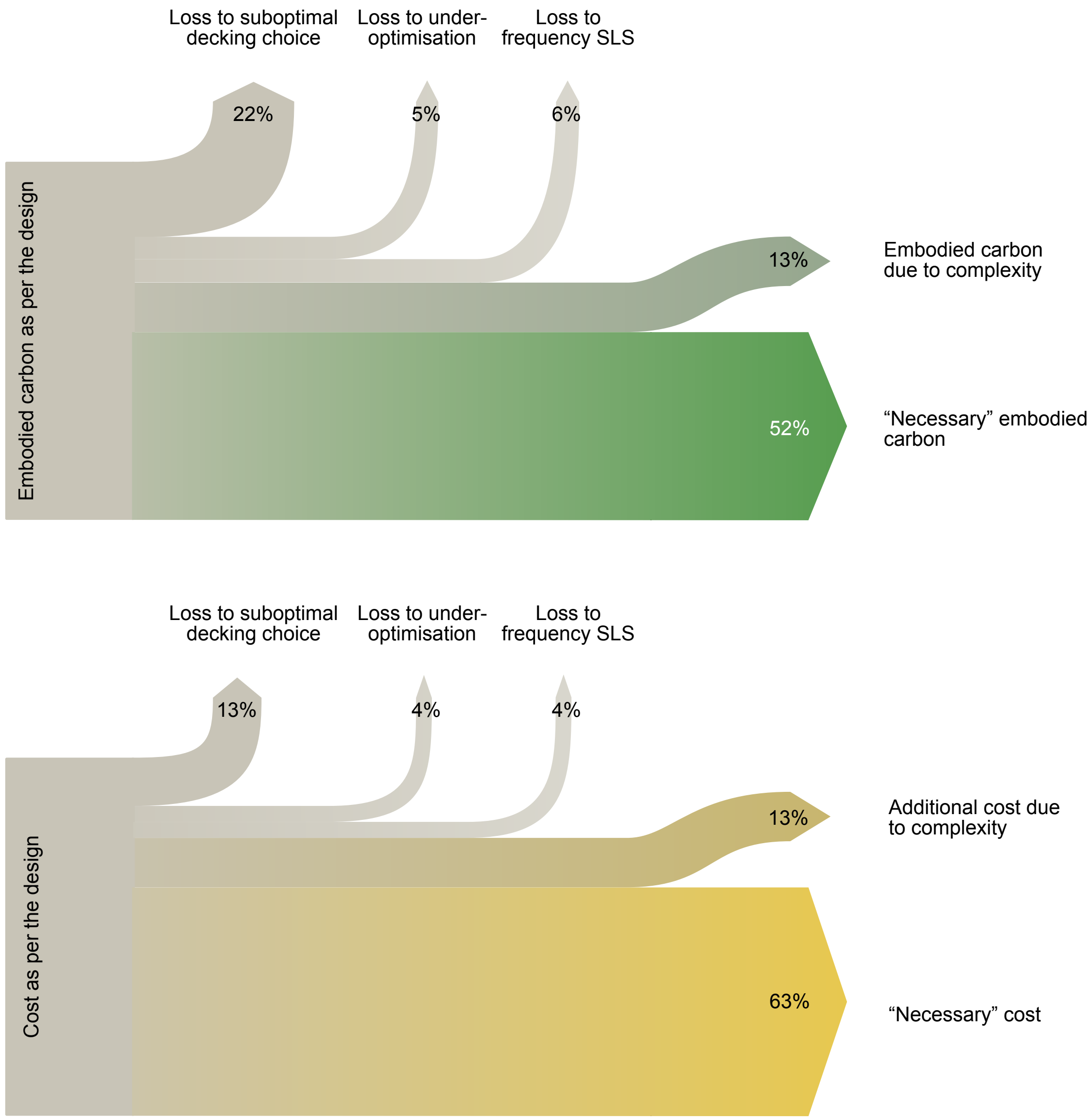

Figure 10: Representation of the losses attributable to various design drivers.

This work was supported by Innovate UK project 'Innovative engineering approach for material, carbon and cost efficiency of steel buildings' ref. 102477; EPSRC Material demand reduction: NMZL/112, RG82144, EPSRC reference: EP/N02351X/1; EPSRC grant EP/P033679/2 and EPSRC programme grant 'UKFIRES' ref. EP/S019111/1;

References

[1] Fridolin Krausmann, Dominik Wiedenhofer, Christian Lauk, Willi Haas, Hiroki Tanikawa, Tomer Fishman, Alessio Miatto, Heinz Schandl, and Helmut Haberl. Global socioeconomic material stocks rise 23-fold over the 20th century and require half of annual resource use. *Proceedings of the National Academy of Sciences*, 2017.

[2] Maria Van der Hoeven and Didier Houssin. Energy technology perspectives 2015: mobilising innovation to accelerate climate action. *International Energy Agency: Paris, France*, 2015.

[3] Jonathan M. Cullen, Julian M. Allwood, and Margarita D. Bambach. Mapping the global flow of steel: From steelmaking to end-use goods. *Environ Sci Technol*, 46(24):13048–13055, 2012.

[4] A Dimoudi and C Tompa. Energy and environmental indicators related to construction of office buildings. *Resour Conserv Recy*, 53(1):86–95, 2008.

[5] Zahra S. Moussavi Nadoushani and Ali Akbarnezhad. Effects of structural system on the life cycle carbon footprint of buildings. *Energ Buildings*, 102:337–346, 2015.

[6] International Energy Agency. Energy technology perspectives 2010: scenarios & strategies to 2050, 2010.

[7] Luisa F Cabeza, Lídia Rincón, Virginia Vilariño, Gabriel Pérez, and Albert Castell. Life cycle assessment (lca) and life cycle energy analysis (lcea) of buildings and the building sector: A review. *Renewable and sustainable energy reviews*, 29:394–416, 2014.

[8] Muiris C. Moynihan and Julian M. Allwood. Utilization of structural steel in buildings. In *Proc. R. Soc. A*, volume 470, page 20140170. The Royal Society, 2014.

[9] Cyrille Francois Dunant, Michal Drewniok, Stathis Eleftheriadis, Jonathan Michael Cullen, and Julian Mark Allwood. Regularity and optimisation practice in steel structural frames in real design cases. *Resources, Conservation & Recycling*, 134:294–302, 2018.

[10] Steve Barg, Forest Flager, and Martin Fischer. An analytical method to estimate the total installed cost of structural steel building frames during early design. *Journal of Building Engineering*, 15:41–50, 2018.

[11] Stathis Eleftheriadis, Cyrille Dunant, Michal Drewniok, William Rogers-Tizard, and Constantinos Kyprianou. Comparative numerical analysis for cost and embodied carbon optimisation of steel building structures. 2018.

[12] M E Brettle and D G Brown. Steel building design: Concise eurocodes. Technical Report P362, The Steel Construction Institute, Silwood Park, Ascot, Berkshire, 2009.

[13] A L Smith, S J Hicks, and P J Devine. Design of floors for vibration:a new approach. Technical Report P354, The Steel Construction Institute, Silwood Park, Ascot, Berkshire, 2009.

[14] W I Simms and A F Hughes. Composite design of steel framed buildings. Technical Report P359, The Steel Construction Institute, Silwood Park, Ascot, Berkshire, 2011.

[15] Rolf Kindmann. Neue berechnungsformel für das it von walzprofilen und berechnung der schubspannungen. *Stahlbau*, 75(5):371–374, 2006.

[16] Cyrille F Dunant, Michał P Drewniok, Michael Sansom, Simon Corbey, Jonathan M Cullen, and Julian M Allwood. Options to make steel reuse profitable: An analysis of cost and risk distribution across the uk construction value chain. *Journal of Cleaner Production*, 183:102–111, 2018.

[17] Various. Platts Steel Price, January 2016.

[18] M Sansom and J Meijer. Life-cycle assessment (lca) for steel construction. *EUR*, (20570):1–160, 2002.

[19] bauforumstahl e.V. Structural steel: Sections and plates. *https://epd-online.com*, (EPD-BFS-20130094-IBG1-EN), 2013.

[20] Ruuki Construction. Structural steel construction products. *https://cdn.ruuki.com*, (EN 15804 ISO 14025), 2014.

[21] SCI. Assessment of the on-site impacts from the construction of steel and concrete structural frames. Technical Report RT 1523, 2013.

[22] BRE. Declaration for carbon steel reinforcing bar (secondary production route —–scrap) sector average. Technical Report BREG EN EPD 000011, 2014.

[23] Skanska Norge. Environmental product declaration; welded plated beams. Technical report, 2014.

[24] Jaakko Haapio. Feature-based costing method for skeletal steel structures based on the process approach. *Tampereen teknillinen yliopisto. Julkaisu-Tampere University of Technology. Publication; 1027*, 2012.

[25] Károly Jármai and Jozsef Farkas. Cost calculation and optimisation of welded steel structures. *Journal of Constructional Steel Research*, 50(2):115–135, 1999.

[26] Davis Langdon. *Spon's Architects' and Builders' Price Book 2005*. Spon Press, 2014.

[27] G Couchman. Minimum degree of shear connection rules for uk construction to eurocode 4. Technical report, The Steel Construction Institute, Silwood Park, Ascot, Berkshire, 2015.

[28] Structural engineers at Price & Meyers. personal communication.

[29] Peter S. P. Wong, Adam Owczarek, Matthew Murison, Zennan Kefalianos, and Joseph Spinozzi. Driving construction contractors to adopt carbon reduction strategies – an australian approach. *Journal of Environmental Planning and Management*, 57(10):1465–1483, 2014.

[30] Peter S.P. Wong, Aiden Lindsay, Lachlan Crameri, and Sarah Holdsworth. Can energy efficiency rating and carbon accounting foster greener building design decision? an empirical study. *Building and Environment*, 87:255 – 264, 2015.

[31] James J Kingman, Konstantinos Daniel Tsavdaridis, and Vassilli V Toropov. Applications of topology optimization in structural engineering: High-rise buildings and steel components. *Jordan Journal of Civil Engineering*, 159(3097):1–23, 2015.

[32] Richard Frans and Yoyong Arfiadi. Sizing, shape, and topology optimizations of roof trusses using hybrid genetic algorithms. *Procedia Engineering*, 95:185–195, 2014.

[33] Fangyi Zhou, Simaan M AbouRizk, and H Al-Battaineh. Optimisation of construction site layout using a hybrid simulation-based system. *Simulation Modelling Practice and Theory*, 17(2):348–363, 2009.

[34] Peter A Irwin. Wind engineering challenges of the new generation of super-tall buildings. *Journal of Wind Engineering and Industrial Aerodynamics*, 97(7-8):328–334, 2009.

[35] Ernst Worrell, Julian Allwood, and Timothy Gutowski. The role of material efficiency in environmental stewardship. *Annual Review of Environment and Resources*, 41:575–598, 2016.

[36] W Shanks, CF Dunant, Michał P Drewniok, RC Lupton, A Serrenho, and Julian M Allwood. How much cement can we do without? lessons from cement material flows in the uk. *Resources, Conservation and Recycling*, 141:441–454, 2019.

Appendix A. List of universal sections considered

203×102×23	152×152×23	203×133×25	305×102×25	305×102×28	254×102×28
203×133×30	152×152×30	254×146×31	305×102×33	356×127×33	254×146×37
305×127×37	152×152×37	406×140×39	356×127×39	305×165×40	305×127×42
254×146×43	356×171×45	406×140×46	203×203×46	305×165×46	356×171×51
457×152×52	203×203×52	406×178×54	305×165×54	406×178×54	457×152×60
406×178×60	203×203×60	457×152×67	457×191×67	406×178×67	356×171×67
203×203×71	254×254×73	457×191×74	406×178×74	457×152×74	533×210×82
457×191×82	457×152×82	533×210×82	406×178×85	203×203×86	457×191×89
254×254×89	533×210×92	305×305×97	457×191×98	533×210×101	610×229×101
610 × 229 × 113	305 × 305 × 118	533 × 210 × 122	686 × 254 × 125	356 × 368 × 153	

$305 \times 305 \times 158$ $610 \times 305 \times 179$ $305 \times 305 \times 198$ $305 \times 305 \times 240$ $914 \times 305 \times 253$ $305 \times 305 \times 283$ $356 \times 406 \times 340$ $914 \times 419 \times 343$ $1016 \times 305 \times 349$ $914 \times 419 \times 389$ $356 \times 406 \times 393$ $1016 \times 305 \times 393$ $1016 \times 305 \times 437$ $356 \times 406 \times 467$ $1016 \times 305 \times 487$ $356 \times 406 \times 551$ $356 \times 406 \times 634$

Table A.7: All decking options used by the analytical model. For each of this option, the model uses the span tables provided by the manufacturer, assuming continuous spans, un-propped construction and 60 minutes for the fire rating.

Name	**Type**
Bison Holocore	Precast
Tata Comflor 46	Composite Trapezoidal
Tata Comflor 51+	Composite Re-entrant
Tata Comflor 60	Composite Trapezoidal
Tata Comflor 80	Composite Trapezoidal
Tata Comflor 100	Composite Trapezoidal
Tata Comflor 210	Composite Trapezoidal
Tata HOLORIB	Composite Re-entrant
Richard Lees Decking E60	Composite Trapezoidal
Richard Lees Decking 80	Composite Trapezoidal
Richard Lees Decking AL	Composite Trapezoidal
Kingspan Multideck 50	Composite Re-entrant
Kingspan Multideck 60	Composite Trapezoidal
Kingspan Multideck 80	Composite Trapezoidal